

1 **FIRST STEPS TO PREDICTING PULP COLOUR IN WHOLE MELONS**
2 **USING NEAR-INFRARED REFLECTANCE SPECTROSCOPY**

3

4 M.T. Sánchez^{a,*}, I. Torres^a, M.J. De la Haba^a, D. Pérez-Marín^{b,*}

5

6

7 ^a *Department of Bromatology and Food Technology, University of Cordoba, Campus of*
8 *Rabanales, 14071 Córdoba, Spain.*

9 ^b *Department of Animal Production, University of Cordoba, Campus of Rabanales,*
10 *14071 Córdoba, Spain.*

11

12

13

14

15

16 **Corresponding authors. Tel.: +34 957 212576; fax: 34 957 212000*

17 *E-mail addresses: teresa.sanchez@uco.es (M.T. Sánchez) or dcperez@uco.es (D. Pérez-*
18 *Marín).*

19

20 **Abstract**

21 NIRS technology was used for the non-destructive measurement of melon-pulp colour
22 (a^* , b^* , C^* and h^*), one of the main indicators of ripeness and quality. A total of 432
23 Cantaloupe and Galia melons were used in the construction of calibration models,
24 testing various spectral signal pretreatments and both linear and non-linear regression
25 algorithms. The coefficient of determination (r^2) and the standard error of cross-
26 validation (SECV) obtained for parameters a^* (0.96, 2.16), b^* (0.85, 3.25), C^* (0.82,
27 3.76) and h^* (0.96, 3.64) in intact fruit confirmed the *a priori* viability of NIRS
28 technology with MPLS regression for measuring melon ripeness and quality. Moreover,
29 the application of a LOCAL algorithm improved the ability of models to predict all the
30 internal-colour quality parameters studied. These results suggest that NIRS technology
31 is a promising tool for monitoring ripening in melons and thus for establishing the
32 optimal harvesting time.

33

34 **Keywords:** near-infrared spectroscopy, melon, internal colour, MPLS regression,
35 LOCAL algorithm.

36

37

38 **1. Introduction**

39 Harvesting melons at the ideal stage is especially critical to their storage life and eating
40 quality. Although sweetness is the key attribute affecting eating-quality, other properties
41 such as aroma, flesh colour and texture—depending on the fruit concerned—are also
42 indispensable indicators of overall quality (Vallone et al., 2013).

43 The quality of muskmelons (*Cucumis melo*) at harvest is traditionally estimated
44 on the basis of a number of subjective external features, chief among which are
45 background colour, net development, and stem abscission (Simandjuntak, Barrett, &
46 Wrolstad, 1996; Portela & Cantwell, 1998; Cantwell & Kasmire, 2002).

47 Cantaloupes may be harvested when the fruit begins to separate from the stem,
48 when the external colour beneath the netting begins to change from green to yellow-
49 green (bearing in mind that skin colour typically transitions from grey to dull green
50 when immature, deep uniform green at maturity, and light yellow at full ripeness), and
51 when the net is well developed with a waxy covering (Cantwell, 1996). To ensure
52 excellent eating quality in melons, it is critical to harvest them at a sufficiently advanced
53 stage when the sugars have already accumulated in the fruit, since postharvest changes
54 in sugar concentrations are small (Pratt, Goeschl, & Martin, 1977; Lester & Shellie,
55 1992). Similarly, although skin colour may change after harvest, pulp colour changes
56 very little, so that harvesting at the appropriate stage of maturity is crucial to good
57 internal visual quality (Cantwell, 1996).

58 Honeydew melons are harvested by maturity, which is very difficult to judge
59 since the abscission zone, a valuable harvest criterion for Cantaloupes, does not form
60 until the fruit is overripe (Pratt, Goeschl, & Martin, 1977). Maturity classes are grouped
61 predominantly by changes in 'ground colour' from greenish to cream with yellow

62 accents. Cantwell (1996) notes that Honeydew melons may be considered mature but
63 unripe when the external colour is white with a greenish aspect, the peel is slightly
64 fuzzy, there is no aroma, when the melon splits when cut, and when the pulp is crisp.
65 They may be classed as mature and ripening when the external colour is white with
66 traces of green, the peel is not fuzzy but slightly waxy, the aroma changes from slight to
67 noticeable, the melon splits when cut and the flesh is crisp. The characteristics of ripe
68 Honeydews are as follows: ground colour is creamy white with yellow accents, peel is
69 clearly waxy, the characteristic aroma is noticeable and the blossom-end yields slightly
70 to pressure. Pratt, Goeschl, & Martin, (1977) report that ripening in Honeydew melons
71 is associated with increased respiration and ethylene production rates, aroma
72 development and softening.

73 The Galia melon is a hybrid originating from a Cantaloupe-Honeydew cross,
74 larger than a Cantaloupe, and with deep green flesh. Ripeness is measured not by
75 softness at the stem but rather by colour and fragrance (Escribano & Lazaro, 2012).

76 Growers and consumers generally estimate melon quality in terms of aroma,
77 softness to the touch and surface colour (Lester, 2006). However, while these are
78 important for establishing product quality and optimal harvesting time, there are other
79 key criteria which cannot be assessed externally, and require non-destructive methods in
80 order to avoid damage to the fruit. Pulp colour is one such criterion: as Cantwell (1996)
81 has noted, fall and winter Cantaloupe melons may be ripe on the inside but have a green
82 peel colour. Cantwell and Portela (1998) highlight the link between pulp colour and
83 surface defects such as sunburned areas and large ground spots (poorly netted areas
84 where melons touch the ground), reporting that average pulp chroma (orange colour)
85 values are highest in good-quality pieces, intermediate in ground-spot pieces, and
86 lowest in pieces from sunburned areas.

87 Growers and the industry would clearly benefit from fast, precise and, above all,
88 non-destructive techniques. NIRS technology not only meets these requirements, but
89 also offers a number of other advantages which make it ideal for meeting current
90 demands in terms of control and traceability: low cost per sample analysed; little or no
91 need for sample preparation; ability to analyse a wide range of products and parameters;
92 a high degree of reproducibility and repeatability; and reduced interference from colour
93 of fruit samples. NIRS can be built into in-line processes, and – since no reagents are
94 required – produces no waste.

95 NIR spectroscopy has been used successfully to predict colour in animal
96 products such as fresh breast muscle (Abeni & Bergoglio, 2001), deboned chicken
97 breast (Liu, Lyon, Windham, Lyon, & Savage, 2004), and beef (Andrés et al., 2008;
98 Prieto, Andrés, Giráldez, Mantecón, & Lavín, 2008; Prieto et al., 2009; Cecchinato, De
99 Marchi, Penasa, Albera, & Bittante, 2011), as well as external colour in mandarins and
100 oranges (Sánchez, De la Haba, Serrano, & Pérez-Marín, 2012; Sánchez, De la Haba, &
101 Pérez-Marín, 2013).

102 Even though the prediction of internal colour is a key factor in establishing
103 optimal harvesting time, no published research appears yet to have addressed this
104 criterion.

105 The overall aim of this study was to evaluate the ability of NIR technology to
106 predict internal colour in melons, a quality parameter strongly influencing consumer
107 acceptance or rejection of the product.

108 **2. Material and methods**

109 **2.1. Fruit samples**

110 A total of 432 melons – N = 220 Cantaloupe (*Cucumis melo* L. var. *reticulatus* Naud.,
111 Vulcano cultivar) and N = 212 Galia (*Cucumis melo* L. var. *reticulatus* Naud., Siglo,

112 Deneb, Esmeralda and Solarking cultivars) – were harvested in glasshouses belonging
113 to the Provincial Fruit and Vegetable Harvesters’ and Exporters’ Association in
114 Almeria, Spain.

115 On arrival at the laboratory, fruit was promptly placed in cold storage, at 5°C and
116 95% relative humidity. Prior to each measurement, fruit samples were left in order to
117 allow the near-surface temperature to stabilize at the laboratory temperature of 20°C.

118 **2.2. Reference data**

119 Internal colour was analysed on the pulp surface using a Minolta Chroma Meter CR-400
120 (Minolta Co. Ltd., Osaka, Japan). Two consecutive readings were taken in the
121 equatorial region of the fruit; readings were averaged for each sample. Colour was
122 expressed as CIELAB (a^* , b^* , C^* , h^*) colour space, where a^* and b^* define red-
123 greenness and blue-yellowness, respectively (CIE, 2004). Chroma (C^*) and hue angle
124 (h^*) were calculated as $(a^{*2} + b^{*2})^{1/2}$ and $\tan^{-1}(b^*/a^*)$, respectively. Illuminant C
125 and 2° standard observer measurements were made in all cases.

126 **2.3. NIR analysis**

127 NIRS analysis was performed using a Perten DA-7000, Flexi-Mode diode array
128 spectrometer (Perten Instruments North America, Inc., Springfield IL, USA), operating
129 between 400-1700 nm with a 5 nm scanning interval.

130 Fruits were scanned using the instrument in the standard upright position.
131 Samples were irradiated from below by the light source. The distance of measurement
132 between the sample and the instrument was 120 mm, with a large, circular surface
133 viewing area (diameter 127 mm). The horizontal distance between the light source and
134 the detectors was 80 mm.

135 Each fruit was placed centrally upon the fruit holder, with the stem-stylar axis
136 horizontal. Three separate spectral measurements were made, after rotating the sample

137 through 120° each time. The three spectra were averaged to provide a mean spectrum
138 for each intact fruit.

139 **2.4. *Spectral repeatability***

140 All chemometric calculations were performed using WinISI software package version
141 1.50 (Infrasoft International, Port Matilda, PA, USA). Spectrum quality was evaluated
142 using the Root Mean Squared (RMS) statistic (Shenk & Westerhaus, 1995a, 1996). This
143 statistic indicates the similarity between different spectra of a single sample, in this case
144 between the three spectra collected per sample. An admissible limit for spectrum quality
145 and repeatability was determined following the procedure described by Martínez,
146 Garrido, De Pedro, & Sánchez (1998) to calculate the standard deviation (STD) limit
147 from the RMS statistic and obtain an RMS cut-off value.

148 **2.5. *Population structuring and detection of spectral outliers prior to calibration***

149 Principal Component Analysis (PCA) was performed on a set of N = 432 samples in
150 order to decompose and compress the data matrix. After PCA, the centre of the spectral
151 population was determined in order to detect outlier samples. The Mahalanobis distance
152 (GH) was calculated between each sample and the centre; samples with a GH value
153 greater than 3 were considered outliers (Shenk & Westerhaus, 1995a). As spectral pre-
154 treatments, the Standard Normal Variate (SNV) plus Detrending (DT) (Barnes, Dhanoa,
155 & Lister, 1989) procedure was used to remove the multiplicative interferences of
156 scatter, and one derivative mathematical treatment was performed: window-wise
157 filtering (1,5,5,1) where the first digit is the order of the derivative, the second is the gap
158 over which the derivative is calculated, the third is the number of data points in a
159 running average or smoothing and the fourth is the second smoothing (Shenk &
160 Westerhaus, 1995b; ISI, 2000).

161 **2.6. *Construction and validation of prediction models by MPLS regression***

162 Once spectral outliers (9 of the original 432 samples) had been removed, a set
163 consisting of 423 samples of the two different melons (Cantaloupe and Galia) was used
164 to construct calibration models. The set was divided into two: a calibration set
165 containing about 75% of the samples (N = 320 samples) and a test set containing the
166 remaining 25% (N = 103 samples) (Table 1). These samples were selected following the
167 method proposed by Shenk and Westerhaus (1991) using the Center algorithm included
168 in the WinISI software to calculate the Global Mahalanobis distance (GH). Samples
169 were ordered based on the Mahalanobis distance to the centre of the population, and
170 three of every four were selected to form part of the calibration set.

171 Modified Partial Least Squares (MPLS) regression (Shenk & Westerhaus,
172 1995a) was tested for the prediction of colour (a^* , b^* , C^* , h^*) in melons in the 535-
173 1650 nm range. Signal noise at the beginning (400-535 nm) and end (1650-1700 nm) of
174 the spectral range was eliminated. To prevent over-fitting, six cross-validation groups
175 were used.

176 For each analytical parameter, various mathematical treatments were evaluated
177 for scatter correction, including the Standard Normal Variate (SNV) and Detrending
178 (DT) methods (Barnes, Dhanoa, & Lister, 1989). Furthermore, four derivate
179 mathematical treatments were tested in the development of NIRS calibrations: 1,5,5,1;
180 2,5,5,1; 1,10,5,1 and 2,10,5,1 (Shenk & Westerhaus, 1995b).

181 The statistics used to select the best equations were: standard error of calibration
182 (SEC), coefficient of determination of calibration (R^2), standard error of cross-
183 validation (SECV), coefficient of determination for cross-validation (r^2), RPD or ratio
184 of the standard deviation of the original data (SD) to SECV, and the coefficient of
185 variation (CV) or ratio of the SECV to the mean value of the reference data for the

186 calibration set. These latter two statistics enable SECV to be standardized, facilitating
187 the comparison of the results obtained with sets of different means (Williams, 2001).

188 The best models obtained for the calibration set, as selected by statistical criteria,
189 were subjected to evaluation using samples not involved in the calibration procedure. A
190 test set composed of 103 samples, not used previously in the model, was evaluated.
191 Models were evaluated following the protocol outlined by Windham, Mertens, &
192 Barton (1989).

193 **2.7. Construction of prediction models using the LOCAL algorithm**

194 For each parameter, an optimization design for the LOCAL algorithm was set up by
195 varying the number of calibration samples (k) from 40 to 100 in steps of 20 and the
196 number of terms (l) from 10 to 14 in steps of 2. This yielded a factorial design of $4 \times 3 =$
197 12 runs. Finally, the number of PLS factors discarded was set to the first four.

198 As in MPLS calibrations, other factors needed to be optimized, including signal
199 pretreatments (light scatter correction and derivatives) and the spectral region used.
200 During LOCAL equation development, the spectral region and signal pretreatments
201 indicated in Section 2.6 were used.

202 The effect of the different settings on the performance of LOCAL was evaluated
203 by comparing the standard error of prediction (SEP), the coefficient of regression for
204 external validation (r^2), the bias, and the bias-corrected standard error of prediction
205 SEP(c). Furthermore, the accuracy of prediction of LOCAL was compared to the SEP,
206 r^2 and bias of MPLS prediction.

207 **3. Results and discussion**

208 **3.1. Spectral repeatability**

209 Optimization of spectrum quality and repeatability is crucial in order to develop robust
210 and accurate models. Statistical methods such as a defined RMS cut-off limit can be

211 useful for this purpose. The RMS cut-off was calculated as indicated in section 2.4. The
212 mean STD for the samples analysed was 62,497 $\mu\log(1/R)$, representing an RMS cut-off
213 of 71,441 $\mu\log(1/R)$. Any sample whose triplicated screening scans yielded an RMS
214 above this value was eliminated and repeated until values fell below that limit, thus
215 ensuring a high degree of spectrum repeatability.

216 No reference to the calculated RMS cut-off value for intact melons has been
217 found in the literature.

218 The mean spectrum of the three replicates of each sample was used for further
219 analysis.

220 **3.2. Spectral features**

221 Typical log (1/R) spectra for intact Cantaloupe and Galia melons, obtained on the
222 Perten DA-7000 instrument, are shown in Fig. 1. The main absorption peaks coincided
223 for both melon varieties at 680 nm, 970 nm, 1190-1210 nm and 1440 nm.

224 In the visible region of the spectrum, absorbance spectra measured on
225 Cantaloupe and Galia melons were similar in shape, with peaks occurring at positions
226 corresponding to known chlorophyll absorption bands: strong absorption by chlorophyll
227 a was evident at 680 nm, with a shoulder at 630 nm due to absorption by chlorophyll b
228 (McGlone, Jordan, & Martinsen, 2002; McGlone, Martinsen, Clark, & Jordan, 2005).
229 Stchur, Cleveland, Zhou, & Michel (2002) report a strong inverse correlation between
230 the presence of this band and fruit sugar content. In addition, red pigments (carotenoids
231 and anthocyanins) have a typical absorption band in the 490 to 550 nm region of the
232 visible spectrum (Strayer, 1995).

233 In the near infrared region, aqueous hydroxyl functional groups were detected at
234 760, 840, 970 and 1440 nm, as is usually the case for fruit, and particularly for melons,

235 which are 90% water (Williams, 2001; McGlone, Martinsen, Clark, & Jordan, 2005).
236 Williams (2001) reports a sugar-related absorption band at around 1200 nm.

237 **3.3. Calibration development**

238 Cross-validation statistics for the best models obtained for the prediction of internal
239 colour (a^* , b^* , C^* and h^*) in intact Cantaloupe and Galia melons using the MPLS
240 algorithm are shown in Table 2.

241 For colour parameter a^* , the MPLS method yielded the best calibrations using
242 D1 log (1/R). Vis-NIR spectroscopy models displayed remarkable predictive ability for
243 this parameter ($r^2 = 0.96$, SECV = 2.16, RPD = 5.30); Shenk & Westerhaus (1996)
244 suggest that an r^2 value greater than 0.9 indicates excellent quantitative information.
245 The RPD (5.30) value demonstrated the robustness and power of the calibration models
246 obtained for a^* .

247 Non-destructive prediction of a^* in melon pulp is highly valuable, since this
248 parameter is linked to pulp carotene—and particularly β -carotene—content (Reid, Lee,
249 Pratt, & Chichester, 1970). During ripening, the pulp attains the maximum orange
250 colour typical of the Cantaloupe melon; a^* is thus a good indicator of maturity in
251 melons (Simandjuntak, Barrett, & Wrolstad, 1996). Conversely, declining a^* values are
252 associated with loss of the typical orange colour hue during storage (Beaulieu, 2005).

253 No references have been found in the literature to the measurement of a^* in the
254 pulp of intact melons using NIRS technology. However, Sánchez, De la Haba, Serrano,
255 & Pérez-Marín (2012) used a diode-array instrument (Corona 45 VIS/NIR, spectral
256 range: 380-1700 nm) and a hand-held MEMS device (Phazir 2400, spectral range:
257 1600-2400 nm) to measure external colour in intact oranges, reporting results poorer
258 than those obtained here (RPD = 1.92 CV = 3.78% for the Corona 45 VIS/NIR; RPD
259 = 1.49, CV = 4.76% for the Phazir 2400).

260 Performance statistics inferior to those recorded here were also obtained by
261 Sánchez, De la Haba, & Pérez-Marín (2013) when using the MEMS spectrophotometer
262 for the on-tree measurement of external colour in mandarins (RPD = 2.04, CV =
263 33.30%).

264 The calibration model displaying the greatest predictive capacity for the b*
265 colour parameter ($r^2 = 0.85$; SECV = 3.25; RPD = 2.61) was obtained using D1 log
266 (1/R); quantification was good, according to the Shenk & Westerhaus (1996)
267 classification.

268 There are no published reports on the measurement of b* in intact melon using
269 NIRS technology, only Sánchez, De la Haba, & Pérez-Marín (2013) reported RPD
270 value of 1.43 and CV value of 4.22% for the prediction of this parameter in intact
271 mandarins using a MEMS instrument in the spectral range 1600-2400 nm. However,
272 this parameter is linked to the behaviour of photosynthetic pigments such as chlorophyll
273 and carotenoids during melon ripening, and may thus act as an indicator of ripeness and
274 thus of optimal harvesting time (Martínez-Madrid, Martínez, Pretel, Serrano, &
275 Romojaro, 1999); non-destructive measurement of b* is therefore of considerable value.

276 As Table 2 shows, good predictive ability ($r^2 = 0.82$; SECV = 3.76; RPD = 2.33)
277 was recorded for the measurement of C* (Shenk & Westerhaus, 1996).

278 Values for C*, like those of a* and b*, increase significantly during ripening,
279 due to higher carotenoid levels, and thus also provide a useful indicator of fruit ripeness
280 (Sánchez, De la Haba, & Pérez-Marín, 2013).

281 The predictive capacity of the best model for the h* colour parameter may be
282 considered excellent ($r^2 = 0.96$, SECV = 3.64, RPD = 5.22) in terms of the
283 recommendations made by Shenk & Westerhaus (1996).

284 Hue angle increases with maturity in melons, indicating a change from light to
285 darker orange in Cantaloupe and a decline in greenness in Galia (Simandjuntak, Barrett,
286 & Wrolstad, 1996).

287 Although NIRS technology appears not to have been used hitherto for measuring
288 C^* and h^* in melons, Sánchez, De la Haba, & Pérez-Marín (2013) used NIRS to
289 measure these colour parameters in on-tree mandarins during ripening, obtaining
290 models whose predictive capacity was inferior to that recorded here both for C^* (RPD =
291 1.68, CV = 7.38%) and for h^* (RPD = 1.31, CV = 9.03%).

292 *3.4. Comparison of internal colour prediction in melons using the LOCAL* 293 *algorithm versus MPLS regression*

294 The LOCAL algorithm was also used to predict internal quality-related parameters, and
295 results for prediction of the 103-sample external validation set were compared with
296 those obtained using MPLS regression.

297 SEP, SEP (c), bias and r^2 values obtained with the best mathematical treatment
298 for each parameter in the 12 runs (3 values for l and 4 for k) are shown in Table 3. The
299 table also shows the combination of k and l yielding the lowest SEP for each parameter
300 ($k = 60$ and $l = 10$ for a^* ; $k = 40$ and $l = 14$ for b^* ; $k = 40$ and $l = 12$ for C^* , $k = 40$ and l
301 = 10 for h^*).

302 For predicting the external validation set, the LOCAL algorithm used only 40
303 samples to predict b^* , C^* and h^* , and 60 samples for a^* ; rather than using all 320
304 samples in the calibration set (as was the case for MPLS regression), only those samples
305 whose spectra were considered representative of the calibration set were used.

306 The results obtained using the LOCAL algorithm were better than those
307 achieved with MPLS regression (Table 3), although both strategies yielded values for

308 the coefficient of determination which were comfortably over the minimum of $r^2 \geq 0.60$
309 recommended by Windham, Mertens, & Barton (1989).

310 For a^* prediction, the LOCAL algorithm improved the coefficient of
311 determination by 2% and reduced the prediction error by 25%. The coefficient of
312 determination for b^* parameter was also improved by about 2% and the prediction error
313 reduced by over 5%.

314 For C^* and h^* , the accuracy and precision of the predictions obtained using the
315 LOCAL algorithm were greater than those obtained using MPLS regression (Table 3).
316 Values for r^2 were improved by 2% and 3%, while prediction error was reduced by 4%
317 and 38%, for C^* and h^* , respectively.

318 Use of the LOCAL algorithm thus yielded a slight improvement in r^2 values for
319 all parameters, as well as minimizing the prediction error for NIRS models constructed
320 to predict internal-colour parameters in melons.

321 **3.5. *Effective wavelengths for predicting colour-related parameters***

322 The loading plots corresponding to the best models obtained for predicting maximum
323 levels of colour parameters are shown in Fig. 2. These plots show the areas across the
324 spectral range where variance has influenced computing of the model to a greater or
325 lesser extent, and the direction of that influence (positive or negative).

326 For predicting a^* , representation of the four latent variables (LV) used in
327 constructing the calibration equation using MPLS regression shows that the areas of the
328 spectrum exerting greatest weight on model fitting were 610 nm, 630 nm, 655 nm, 685
329 nm and 725 nm in the visible region, and the 950 nm and 1410 nm areas relating to the
330 absorption of sugars and water (Fig. 2). The same areas exerted greatest weight for
331 parameter b^* (Fig. 2).

332 For chroma (C^*), peaks and valleys were observed in similar areas: 610 nm, 630
333 nm, 655 nm, 685 nm, and 725 nm, in addition to 950 nm and 1410-1480 nm (Fig. 2).

334 For h^* , the most significant wavelengths were 615 nm, 625 nm, 655 nm, 685 nm
335 and 725 nm in the visible region, together with 950 nm, 1225 nm, 1415 nm and 1480
336 nm, areas related to sugar and water absorption; their influence was either positive or
337 negative, depending on the latent variable in question (Fig. 2).

338 Thus, wavelengths 630, 680, 725, 950, and 1410 nm are likely to be the most
339 sensitive for colour-related parameters in intact melons.

340 **4 Conclusions**

341 NIRS technology, using a diode array spectrometer, proved to be suitable for assessing
342 internal colour-related parameters in the pulp of intact melons, allowing ripeness to be
343 evaluated not only in terms of external visual appearance but also in terms of internal
344 colour. This could lead to major changes in harvesting techniques for melons, by
345 providing farmers with a precise and accurate indication of the fruit's internal quality,
346 thus enabling selective harvesting. It must be highlighted that the results obtained here
347 should be considered the first step in the fine-tuning of NIRS for monitoring the
348 ripening process in melons. Over the coming years, recalibrations may be required in
349 order to enhance the robustness of the models obtained.

350 **Acknowledgements**

351 This research was funded by the Andalusian Regional Government under the Research
352 Excellence Program (Project No. 3713 'Safety and Traceability in the Food Chain using
353 NIRS'). The authors thank Ms Katherine Flores-Rojas for her technical assistance.

354 **References**

355 Abeni, F., & Bergoglio, G. (2001). Characterization of different strains of broiler
356 chicken by carcass measurements, chemical and physical parameters and NIRS
357 on breast muscle. *Meat Science*, 57, 133-137.

358 Andrés, A., Silva, A., Soares-Pereira, A. L., Martins, C., Bruno-Soares, A. M., &
359 Murray, I. (2008). The use of visible and near infrared reflectance spectroscopy
360 to predict beef *M. longissimus thoracis et lumborum* quality attributes. *Meat*
361 *Science*, 78, 217-224.

362 Barnes, R. J., Dhanoa, M. S., & Lister, S. J. (1989). Standard Normal Variate
363 Transformation and De-trending of near infrared diffuse reflectance spectra.
364 *Applied Spectroscopy*, 43, 772-777.

365 Beaulieu, J. C. (2005). Within-season volatile and quality differences in stored fresh-cut
366 Cantaloupe cultivars. *Journal of Agricultural and Food Chemistry*, 53, 8679-
367 8687.

368 Cantwell, M. (1996). Case study: quality assurance for melons. *Perishables Handling*
369 *Newsletter Issue*, 85, 10-12.

370 Cantwell, M., & Portela, S. (1998). The importance of raw material quality for fresh-cut
371 products: the impact of melon defect as an example. *Perishables Handling*
372 *Quarterly Issue*, 96, 2-3.

373 Cantwell, M., & Kasmire, R. E. (2002). Postharvest handling systems: Fruit vegetables.
374 In A. Kader (Ed.), *Postharvest technology of horticultural crops* (pp. 407-421).
375 Oakland, California: University of California, Division of Agriculture and
376 Natural Resources.

377 Cecchinato, A., De Marchi, M., Penasa, M., Albera, A., & Bittante, G. (2011). Near-
378 infrared reflectance spectroscopy predictions as indicator traits in breeding

379 programs for enhanced beef quality. *American Society of Animal Science*, 89,
380 2687-2695.

381 CIE. (2004). *Colorimetry*. (3rd ed.). Vienna: Commission Internationale De L'Eclairage.

382 Escribano, S., & Lazaro, A. (2012). Sensorial characteristics of Spanish traditional
383 melon genotypes: has the flavour of melon changed in the last century?
384 *European Food Research and Technology*, 234, 581-592.

385 ISI. (2000). *The complete software solution using a single screen for routine analysis,*
386 *robust calibrations and networking*. Manual. FOSS NIRSystems/Tecator. Silver
387 Spring, MD: Infrasoft International.

388 Lester, G. (2006). Consumer preference quality attributes of melon fruits. *Acta*
389 *Horticulture*, 712, 175–182.

390 Lester, G., & Shellie, K. C. (1992). Postharvest sensory and physicochemical attributes
391 of Honeydew melon fruits. *HortScience*, 27, 1012-1014.

392 Liu, Y., Lyon, B. G., Windham, W. R., Lyon, C. E., & Savage, E. M. (2004). Prediction
393 of physical, colour and sensory characteristics of broiler breasts by Visible/Near
394 Infrared Reflectance Spectroscopy. *Poultry Science*, 83, 1467-1474.

395 Martínez, M. L., Garrido, A., De Pedro, E. J., & Sánchez, L. (1998). Effect of sample
396 heterogeneity on NIR meat analysis: The use of the RMS statistic. *Journal of*
397 *Near Infrared Spectroscopy*, 6, 313–320.

398 Martínez-Madrid, M. C., Martínez, G., Pretel, M. T., Serrano, M., & Romojaro, F.
399 (1999). Role of ethylene and abscisic acid in physicochemical modifications
400 during melon ripening. *Journal of Agricultural and Food Chemistry*, 47, 5285-
401 5290.

402 McGlone, V. A., Jordan, R. B., & Martinsen, P. J. (2002). Vis/NIR estimation at harvest
403 of pre and post-storage quality indices for Royal Gala apple. *Postharvest*
404 *Biology and Technology*, 25, 135-144.

405 McGlone, V. A., Martinsen, P. J., Clark, C. J., & Jordan, R. B. (2005). On-line detection
406 of Brownheart in Braeburn apples using near infrared transmission
407 measurements. *Postharvest Biology and Technology*, 37, 142-144.

408 Portela, S. I., & Cantwell, M. I. (1998). Quality changes of minimally processed
409 Honeydew melons stored in air or controlled atmosphere. *Postharvest Biology*
410 *and Technology*, 14, 351-357.

411 Pratt, H. K., Goeschl, J. D., & Martin, F. W. (1977). Fruit growth and development,
412 ripening, and the role of ethylene in the 'Honeydew' muskmelon. *Journal*
413 *American Society Horticultural Science*, 102, 203-210.

414 Prieto, N., Andrés, S., Giráldez, F. J., Mantecón, A. R., & Lavín, P. (2008). Ability of
415 near infrared reflectance spectroscopy (NIRS) to estimate physical parameters of
416 adult steers (oxen) and young cattle meat samples. *Meat Science*, 79, 692-699.

417 Prieto, N., Ross, D. W., Navajas, E. A., Nute, G. R., Richardson, R. I., Hyslop, J. J.,
418 Simm, G., & Roehe, R. (2009). On-line application of visible and near infrared
419 reflectance spectroscopy to predict chemical–physical and sensory
420 characteristics of beef quality. *Meat Science*, 83, 96-103.

421 Reid, M. S., Lee, T. H., Pratt, H. K., & Chichester, C. O. (1970). Chlorophyll and
422 carotenoid changes in developing muskmelons. *Journal American Society*
423 *Horticultural Science*, 95, 814-815.

424 Sánchez, M. T., De la Haba, M. J., & Pérez-Marín, D. (2013). Internal and external
425 quality assessment of mandarins on-tree and at harvest using a portable NIR
426 spectrophotometer. *Computers and Electronics in Agriculture*, 92, 66-74.

427 Sánchez, M. T., De la Haba, M. J., Serrano, I., & Pérez-Marín, D. (2012). Application
428 of NIRS for nondestructive measurement of quality parameters in intact oranges
429 during on-tree ripening and at harvest. *Food Analytical Methods*, 6, 826-837.

430 Shenk, J. S., & Westerhaus, M. O. (1991). Population structuring of near infrared
431 spectra and modified partial least squares regression. *Crop Science* 31, 1548-
432 1555.

433 Shenk, J. S., & Westerhaus, M. O. (1995a). *Analysis of agriculture and food products*
434 *by near infrared reflectance spectroscopy*. Monograph. Silver Spring, MD:
435 NIRSystems, Inc.

436 Shenk, J. S., & Westerhaus, M. O. (1995b). *Routine operation, calibration, development*
437 *and network system management*. Manual. Silver Spring, MD: NIRSystem, Inc.

438 Shenk, J. S., & Westerhaus, M. O. (1996). Calibration the ISI way. In A. M. C. Davies,
439 & P. C. Williams, (Eds.), *Near infrared spectroscopy: the future waves* (pp 198-
440 202). Chichester: NIR Publications.

441 Simandjuntak, V., Barrett, D. M., & Wrolstad, R. E. (1996). Cultivar and maturity
442 effects on muskmelon (*Cucumis melo*) color, texture, and cell wall
443 polysaccharide composition. *Journal of the Science of Food and Agriculture*, 71,
444 282-290.

445 Stchur, P., Cleveland, D., Zhou, J., & Michel, R. G. (2002). A review of recent
446 applications of near infrared spectroscopy, and of the characteristics of a novel
447 PbS CCD array-based near-infrared spectrometer. *Applied Spectroscopy Reviews*
448 37, 383-428.

449 Strayer, L. (1995). *Biochemistry*. (4th ed.). New York: W.H. Freeman and
450 Company/Worth Publishers.

451 Vallone, S., Sivertsen, H., Anthon, G. E., Barrett, D. M., Mitcham, E. J., Ebeler, S. E.,
452 & Zakharov, F. (2013). An integrated approach for flavour quality evaluation in
453 muskmelon (*Cucumis melo* L. *reticulatus* group) during ripening. *Food*
454 *Chemistry*, 139, 171-183.

455 Williams, P. C. (2001). Implementation of near-infrared technology. In P. C. Williams,
456 & K. H. Norris (Eds.), *Near-infrared technology in the agricultural and food*
457 *industries* (pp. 145-169). St. Paul, Minnesota: AACC, Inc.

458 Windham, W. R., Mertens, D. R., & Barton II, F. E. (1989). Protocol for NIRS
459 calibration: sample selection and equation development and validation. In G. C.
460 Martens, J. S. Shenk, & F. E. Barton II (Eds.), *Near infrared spectroscopy*
461 *(NIRS): analysis of forage quality. Agriculture handbook*, vol. 643 (pp. 96–
462 103). Washington, DC: US Government Printing Office.

463

464 Table 1 - Range, mean, standard deviation (SD) and coefficient of variation (CV) for the
 465 parameters studied in calibration ($N_{\text{Calibration}} = 320$) and validation ($N_{\text{Validation}} = 103$) sets.
 466

Parameter	Set	Range	Mean	SD	CV (%)
a*	Calibration	-19.56-18.91	1.99	11.55	580.40
	Validation	-14.56-17.17	2.32	11.62	500.86
b*	Calibration	12.98-50.67	33.36	8.52	25.54
	Validation	13.53-47.19	33.77	8.89	26.33
C*	Calibration	13.51-53.44	35.27	8.87	25.15
	Validation	13.99-49.78	35.68	9.24	25.90
h*	Calibration	66.11-125.11	90.81	19.06	20.99
	Validation	69.07-114.87	90.37	19.08	21.11

467

468 Table 2 - Calibration statistics for the best equations obtained for the prediction of
 469 internal pulp colour (a*, b*, C* and h*) in Cantaloupe and Galia melons.

Parameter	Mathematical treatment	Mean	SD	Range	SEC	R ²	SECV	r ²	RPD	CV
a*	1,5,5,1	2.19	11.44	-14.26-18.66	1.96	0.97	2.16	0.96	5.30	98.63
b*	1,5,5,1	33.49	8.48	12.98-47.40	2.96	0.88	3.25	0.85	2.61	9.70
C*	1,5,5,1	35.35	8.76	13.51-50.77	3.40	0.85	3.76	0.82	2.33	10.63
h*	1,5,5,1	90.63	18.99	67.16-115.62	3.29	0.97	3.64	0.96	5.22	4.01

470

471

472 Table 3 - Validation statistics for the best models for predicting internal colour in
 473 Cantaloupe and Galia melons using MPLS and LOCAL algorithms.

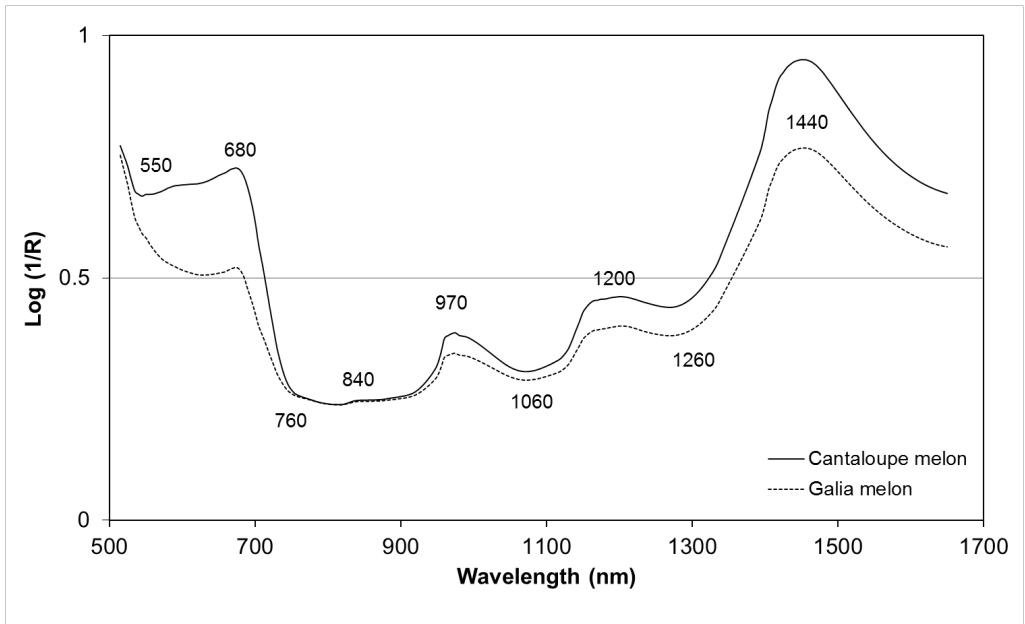
Parameter	Regression method	Mathematic treatment	Factors	SEP	Bias	SEP (c)	r ²	Slope
a*	MPLS	1,5,5,1	15	2.45	-0.25	2.45	0.96	1.00
	LOCAL (k = 60)	1,5,5,1	10 (-4)	1.84	-0.01	1.85	0.98	1.02
b*	MPLS	1,5,5,1	14	3.33	0.46	3.31	0.86	0.96
	LOCAL (k = 40)	1,5,5,1	14 (-4)	3.12	-0.15	3.13	0.88	1.03
C*	MPLS	1,5,5,1	14	3.64	0.30	3.65	0.84	0.96
	LOCAL (k = 40)	1,5,5,1	12 (-4)	3.45	-0.14	3.47	0.86	1.03
h*	MPLS	1,5,5,1	14	3.74	0.30	3.74	0.96	0.97
	LOCAL (k = 40)	1,5,5,1	10 (-4)	2.31	0.30	2.30	0.99	1.01

474

475

476 **Fig. 1 - Typical log (1/R) spectra for Cantaloupe and Galia melons.**

477



478

479

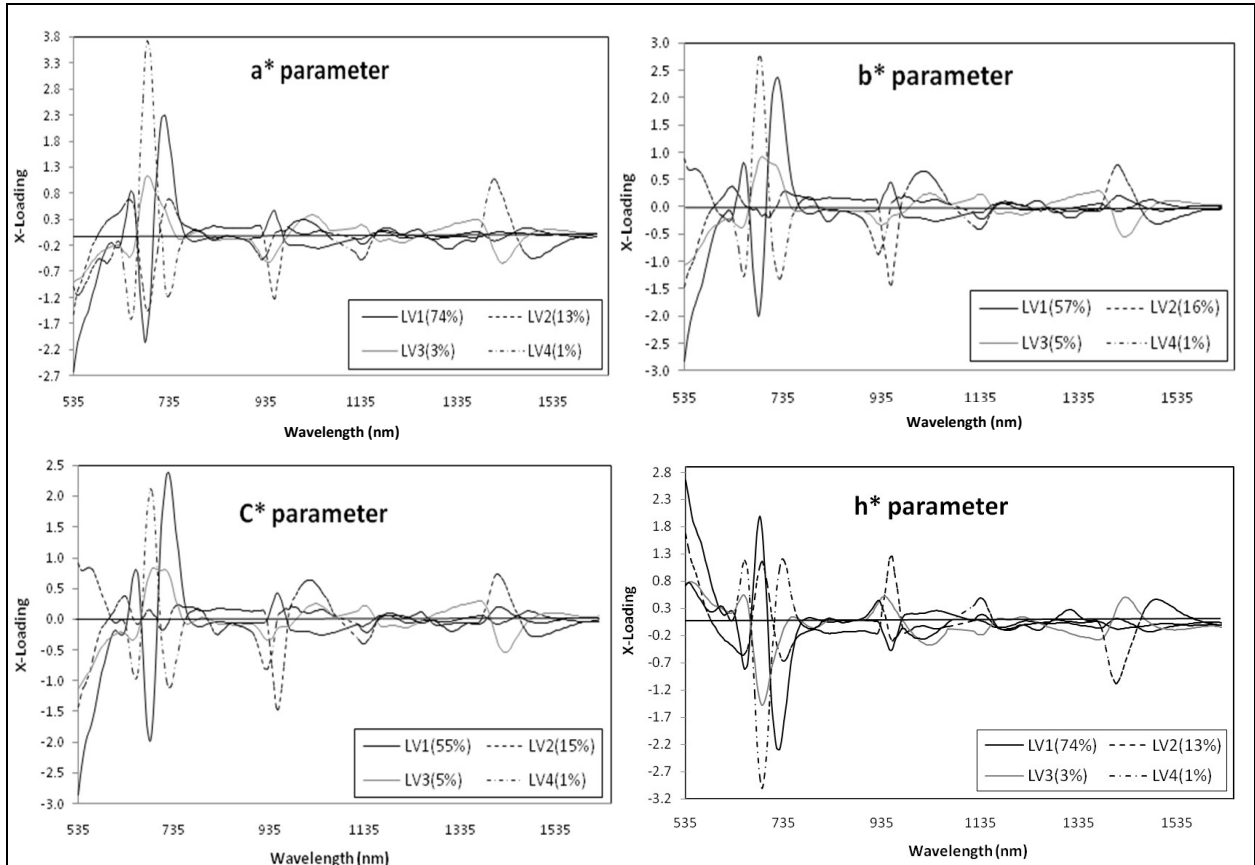
480

481

482

483 **Fig. 2 - Loadings for internal colour related parameters of Cantaloupe and Galia**
484 **melons.**

485



486